Informes Técnicos Ciemat **967**
Junio, 2001

# Glasses, Coatings, Glues and Gamma-ray Irradiation

CIEMAT
J. M. Barcala
M.G. Fernández
A. Ferrando
J. Fuentes
M. I. Josa
A. Molinero
J. C. Oller

CESIC
P. Arce
E. Calvo
C.F. Figueroa
T. Rodrigo
I. Vila
A. L. Virto

CIDA
J.M. Beigveder
I. Génova
G. Pérez
J.A. Ruiz

**Departamento de Fusión y Física de Partículas Elementales**

Toda correspondenica en relación con este trabajo debe dirigirse al Servicio de Información y Documentación, Centro de Investigaciones Energéticas, Medioambientales y Tecnológicas, Ciudad Universitaria, 28040-MADRID, ESPAÑA.

Las solicitudes de ejemplares deben dirigirse a este mismo Servicio.

Los descriptores se han seleccionado del Thesauro del DOE para describir las materias que contiene este informe con vistas a su recuperación. La catalogación se ha hecho utilizando el documento DOE/TIC-4602 (Rev. 1) Descriptive Cataloguing On-Line, y la clasificación de acuerdo con el documento DOE/TIC.4584-R7 Subject Categories and Scope publicados por el Office of Scientific and Technical Information del Departamento de Energía de los Estdos Unidos.

Depósito Legal: M-14226-1995
ISSN: 1135-9420
NIPO: 402-01-008-3

Editorial CIEMAT

CLASIFICACIÓN DOE Y DESCRIPTORES

S70
LINEAR COLLIDERS; LASERS; BEAMS; GAMMA RADIATION; GLASS; COATINGS; ALIGNEMENT; STELLARATORS.

# Glasses, Coatings, Glues and Gamma-ray Irradiation

Barcala, J.M.; Fernández, M.G.; Ferrando, A.; Fuentes, J.; Josa, M.I.; Molinero, A.; Oller, J.C.
CIEMAT* (Madrid, Spain)
Arce, P.; Calvo, E.; Figueroa, C.F.; Rodrigo, T.; Vila, I.; Virto, A.L.
Instituto de Física de Cantabria. CSIC-University of Cantabria ** (Santander, Spain)
Beigveder, J.M.; Génova, I.; Pérez, G.; Ruiz, J.A.
CIDA (Madrid, Spain)

28 pp. 11 fig. 11 refs.

## Abstract:

Most of the alignment systems for LHC experiments use optomechanical elements conforming a network of points that are monitored by laser beams. LHC experiments, working at the expected nominal luminosity, will induce an extremely high irradiation. Basic components such as glasses, coatings and glues may change and their performance may degrade significantly. We have tested various components and identified some of them that can stand 10 years of LHC operation.

# Vidrios, Recubrimientos, Adhesivos e Irradiación con Rayos-gamma

Barcala, J.M.; Fernández, M.G.; Ferrando, A.; Fuentes, J.; Josa, M.I.; Molinero, A.; Oller, J.C.
CIEMAT* (Madrid, Spain)
Arce, P.; Calvo, E.; Figueroa, C.F.; Rodrigo, T.; Vila, I.; Virto, A.L.
Instituto de Física de Cantabria. CSIC-University of Cantabria ** (Santander, Spain)
Beigveder, J.M.; Génova, I.; Pérez, G.; Ruiz, J.A.
CIDA (madrid, Spain)

28 pp. 11 fig. 11 refs.

## Resumen:

La mayor parte de los sistemas de alineamiento en experimentos LHC usarán elementos optomecánicos formando una red de puntos monitorizados por láseres. Los experimentos LHC, trabajando a la luminosidad nominal, provocarán una fuerte irradiación. Componentes básicos tales como vidrios, sus eventuales recubrimientos y adhesivos pueden sufrir cambios y sus prestaciones verse seriamente degradadas. Hemos probado los efectos de la irradiación gamma en varios componentes e identificado algunos que no se verán afectados tras 10 años de operación del LHC.

*Under CICYT (Spain) grant: AEN 99-0312. ** Under CICYT (Spain) grant: AEN 99-0571

# 1 Introduction

The CMS [1] Link Alignment System [2], is designed to relate the position of the CMS inner Tracker [3] and the Muon System [2]. Tracker and Muon chambers are the CMS detectors allowing the space reconstruction of charged particles in the pseudorapidity range ±3, equivalent to a polar angle $\Theta = \pm 5.7$ arc. deg.

In the space regions in the $|\eta| = 3$ neighbourhood the irradiation will be as high as 10 kGy/year at the LHC nominal luminosity of $10^{34}$ $cm^{-2}$ $s^{-1}$. Among the components of the link system there will be some optical pieces, located at $|\eta| = 3$, that should stay transparent in spite of the high radiation.

In the laser source units, rhomboid section prisms are glued to right angle prisms, to split and shift the incoming light ray. The light crosses the whole inside of the piece and, not only the glass should remain transparent, but, in addition, the glue should not degrade, to avoid undesired motions between glued pieces.

To reach the inner tracker, by the outer side, the light path changes its direction twice by means of a periscope formed by a splitter and a mirror, both glued to a rigid bar of fused silica.

2D semitransparent amorphous silicon sensors are used to tag spatial positions of the beam light. Some of them will also be located in the difficult $|\eta| = 3$ space regions, and one has to guarantee that their optical properties will not change with the irradiation.

To check the radiation resistance of the most compromised link alignment components we have proceeded to irradiate them and to check eventual changes in performance.

The irradiation of the amorphous silicon sensors has been the subject of a previous article [4]. The present work deals with the behaviour of glasses, coatings and glues under irradiation with gamma-rays from $^{60}$Co sources.

The paper is organised as follows. An introduction to the CMS link alignment system is done in section 2, where the elements subject to irradiation are presented. Section 3 is devoted to the consequences of irradiation on glass transmittance, while effects on coatings are discussed in section 4. With respect to gluing, we will concentrate on eventual deformation effects that will induce uncontrolled changes in the laser beam direction or in the light transmittance. This is treated in section 5. Finally, the summary and conclusions are found in section 6.

# 2 The CMS link alignment system

The Link System connects Muon and Tracker detectors by creating six light paths joining them. The light paths define planes in $\Phi$ every 60°. Fig. 1 shows a longitudinal cut of the CMS experiment showing a $\Phi$ plane, with the layout of the link alignment lines. As seen in the figure and to minimise the interference with other sub-detectors, the light path follows the inner detector boundaries. The location of the link points along the path are also indicated in Fig. 1.

At each $\Phi$ plane, the light beams are generated by two independent laser sources, or laser boxes, located at $z \approx \pm$ 6635 mm, $r \approx$ 627 mm and attached to the end-cap return yoke. Each source produces two laser beams at fixed angle of about 95.7°. At the inner detector part along the end-cap detector boundaries, the optical lines are parallel to $|\eta| = 3$ and reach the tracker at r ≈ 300 mm. On the tracker alignment wheels, radial periscopes shift the light path from $|\eta| = 3$ to match the alignment passages at the outer radius boundaries of the inner tracker detector, allowing optical measurements across this volume. Fig. 2 gives an scheme of the light path linking central tracker and muon chambers and the location of the various optic-mechanical components, cited above, for one quarter of a $\Phi$ plane.

## 2.1 The laser box

The laser box contains a laser source that sends a light ray to a splitter. One of the outgoing rays goes to the tracker and the other one enters on an optical object consisting on a rhomboid prism coupled to a right angle prism. A sketch of the laser box optics is shown in Fig. 3. The incoming beam is in part reflected by one of the rhomboid faces and in part goes through the glass and comes out in turn reflected by the second face of the rhomboid prism. In that way, the two outgoing beams are parallel, one in the direction of the barrel muon chambers and the other one for linking the end-cap muon chambers.

From the point of view of irradiation effects, it is necessary that the glasses do not get coloured, since the light goes through the splitter and the modified rhomboid prism. On the other hand, the glue (used in the rhomboid prism/right angle prism interface) should not change its optical properties, neither suffer deformations giving rise to rotations of the coupled pieces. The direction of any of the three beam lights going out from the laser box should not change in more than 20 μrad because of the irradiation of glues and glasses.

## 2.2 The periscope

The periscope (see drawings for a prototype in Fig. 4) is composed of three elements: a planeparallel glass layer to split the incoming beam light, a mirror and a support bar. Splitter and mirror are glued to the bar with very precise angles with respect to the incoming beam. The laser light (that comes from the splitter of the laser box) first arrives to the splitter. The refracted ray should reach a position detecting sensor while the reflected one should arrive to the mirror and be reflected to enter in the tracker.

Once more, the irradiation should not affect the direction of the light transmitted and/or reflected because of eventual changes of the optical/mechanical properties of the glasses, coatings and glues.

# 3 The effect of the irradiation on glasses

We have irradiated with gamma-rays, using Cobalt sources, four different type of glasses: BK7, BK7-G18, fused silica and optical grade fused silica (Synthetic Quartz). The irradiation was done at the NAYADE facility of CIEMAT (Spain).

The four glasses were irradiated up to a total dose of 100 kGy, equivalent to 10 years of use in CMS, at the nominal luminosity of LHC and for glasses located at $|\eta| \approx 3$.

As a result of the irradiation, the BK7 probe went from transparent to absolutely black. The fused silica became grey.

On the contrary, BK7-G18 and Synthetic Quartz do not degrade in excess their optical properties. As an example we show in Fig. 5 the transmittance and the reflectance, as a function of the incoming light wave length (in the visible: 436 nm - 900 nm), of two probes of synthetic quartz, one irradiated and the other one non irradiated. Left scale refers to the transmittance and right scale to the reflectance.

Measurements were done with a Palmer-Elmer Lambda 9 spectrophotometer at CIDA (Spain). The degradation in the transmittance stays always below 0.5 %. A slight increase in the reflectance, in agreement with the small lose in transparency, can also be seen.

The measurements (not shown) done in the UV range reveal a degradation in transmittance of up to 15%, while no change (< 0.5%) is observed in the IR.

## 4 The effect of the irradiation on coatings

In the glasses that have to be traversed by the light beams, the transmittance has to be maximised and very often are protected with an anti-reflecting coating. For the tests we have used layers of BK7-G18 as substrate. The dose was 100 kGy as in section 3.

The effect of the irradiation on a standard triple anti-reflecting coating is shown in Fig. 6, where transmittance and reflectance are given as a function of the incoming light wave-length (for the visible). No appreciable change in transmittance, nor in reflectance, is detected.

## 5 The effect of the irradiation on glues

Some components of crucial optical elements as the laser boxes or the periscopes are attached among them by gluing. As already pointed out, the glue joining the components should not degrade, to avoid undesirable motions that would contribute to the beam instability.

We have built some glass-glued objects, irradiated them with photons and measured the eventual degradation of the glue (formation or increment of wedges). The measurements are done by mechanical and optical methods.

### 5.1 Mechanical measurements

We have constructed two retro-reflector type objects in BK7, each consisting on two right angle prisms glued to the two extremes of a rectangular prism, as shown in Fig. 7. We have used a co-ordinates measuring machine DEA (Digital Electronic Automation Inc.). Manually operated, DEA is a vertical bridge-type machine capable of making measurements in three orthogonal axes

The machine has about 5 $\mu$m resolution in each of the 3 co-ordinates. We use it to define the two inclined planes of the retro-reflector and calculate the angle that the two normals form in space (see Fig. 7). By construction, the angle will be close to $\pi/2$. One of the retro-reflectors was glued with LOCTITE 350 and the other with NOA61 (Epotecny).

The DEA machine works by contact: one pin (see photographs on Fig.8) touches one of the inclined faces and takes 9 points over the whole surface. The normal to the plane is then calculated. Then, the pin moves to the second plane and repeats the operation. The procedure is repeated as to obtain 20 pairs of normals that are combined among them as to obtain 400 independent measurements of the angle in the space between both normals. The results, for both probes are given in table 1.

The difference in time between measurements, even for the same dose and the same object, was of several months, to avoid repetition of environmental conditions. The two first lines in table 1 correspond to measurements before irradiation. The r.m.s. of the corresponding distributions are also given in Table 1.

After the first 100 kGy of gamma-ray dose we observed a change of the angle distributions for both types of glues. In the case of LOCTITE the angle varies by 46 μrad, and 56 μrad for NOA61. The change in angle may correspond to a deformation of the thin glue layers.

To try to confirm that the change is related to the irradiation, we have given a second 100 kGy gamma-ray dose to the object glued with NOA61 and then proceeded to a new measurement of the angles in both retroreflectors. Fourth line in Table 1 shows that the mean value for LOCTITE 350 remains compatible with previous value (as expected, as this probe did not get a second 100 kGy dose), while the mean value for the NOA61 object has moved by 30 μrad in the same direction before.

Although they are of the same order than the measurement errors we may claim we are observing real motions of the glued prisms, the glue may be getting wedges that modified the measured angle. On the other hand, the glass itself may have deformed (it was transparent before the irradiation and black after the first 100 kGy).

These two reasons led us to proceed with optical measurements, that, in principle, should be more accurate.

## 5.2 Optical measurements

We prepared 4 probes made of BK7-G18, consisting in glued pairs of circular glasses, each layer being of about 13 mm section and 1.5 mm thick, and 4 other probes made of Synthetic Quartz, consisting on glued pairs of squared glasses, each layer having about 15 mm side and 1.5 mm thickness. For the eight pairs of glasses the wedge $\Delta\alpha$ (see sketch in Fig. 9) between both glasses, before and after gamma-irradiation, was measured with a gonio/spectrometer VIS.

The Gonio/Spectrometer VIS consists of a goniometer for precision measurements of angles and a group of spectral lamps allowing measurements in the visible range.

The measuring process, using a CCD camera, is based on the autocollimator method. This is an optical method for checking and measuring very small angular deviations. A small change in the angle between the optical axis of the autocollimator and the surface in test results in a measurable widening of the autocollimator image.

The autocollimator telescope projects the image of a reticule in a parallel beam (collimated beam) onto the surface in test, which reflects the beam back into the autocollimator. This is the autocollimator image.

If the surface in test is perpendicular to the optical axis, the beam is reflected back into itself. If the surface in test is tilted through an angle $\Delta\alpha$, the reflected beam falls into the autocollimator lens with an angle $\alpha$. Depending on the inclination of the reflected beam, the autocollimator image is displaced in a grater or lesser degree.

The rotation of the autocollimator on the goniometer axis provides a measurement of the angular displacement of the autocollimator image, allowing to obtain the angle $\Delta\alpha = 180 - \alpha$.

Errors given in Tables 2 and 3 for each measurement point were calculated in accordance with CIDA requirements and following the "Guide to the expression of uncertainty in measurement" (ISO 1995). The reported uncertainty is the extended uncertainty of measurement obtained by multiplying the standard uncertainty by a save factor 2, providing about 95% confidence level.

We have evaluated the following glues: Epotecny NOA61, LOCTITE 15 8350 16992, MELTMOUNT (60°, 1' UVA at 20 cm) and a current technique of molecular adhesion in vacuum (VACUUM).

The applied gamma-ray dose was, in all cases, 150 kGy, in steps of 50 kGy. Measurements of the wedges sizes and of the light transmittance, in the visible, were done before irradiation and after each irradiation step.

Table 2 summarises the results for the BK7-G18 probes. The ones glued with NOA61, LOCTITE and using the VACUUM technique, do not change the size of their respective wedges after the three 50 kGy doses. However, the probe glued with MELTMOUNT seems to change the size of the wedge by about 35 μrad after the first 50 kGy dose. No further change was observed after the next two 50 kGy doses.

Results for the Synthetic Quartz probes are shown in Table 3. For this glass, small wedge size changes, compatible with the measurement uncertainties, are observed for the probes with LOCTITE, MELTMOUNT and VACUUM. For NOA61 a change of about 19 μrad ($3\sigma$ significance) is seen after the first 50 kGy dose, not evolving any further after the subsequent irradiations.

Light transmittance (in the range 400 - 900 nm) was measured, as said, in all the eight probes, before irradiation and after each of the 50 kGy dose, using the CIDA Palmer Elmer spectrophotometer. Beam light has 5 mm height and is 1.8 mm broad. The results are shown in Figs. 10 and 11, for the BK7G18 and Synthetic Quartz probes, respectively.

Concerning BK7G18 probes, we observe a shift of the absorption edge at low wave length after the first irradiation dose. This effect can be seen in the VACUUM probe as well as in the other three, indicating that the effect is due to changes in the absorption edge of the glass and has nothing to do with eventual changes in the glues. After the two next irradiation steps we do not observe any appreciable change in transmittance.

Concerning Synthetic Quartz probes, and for those where glue is used, we observe a tendency of the spectra to get bended at low wave-lengths when accumulating irradiation doses. This effect is most probably due to changes in the glue, since it is not seen in the VACUUM probe.

In all cases, the transmittance stays above the 90% without any significant (< 1%) change in properties. This means that neither the glasses nor the glues form coloured centres due to the irradiation. Notice that the total gamma-ray dose, 150 kGy, is equivalent to 15 years of CMS operation.

## 6 Summary and conclusions

We have investigated the effects of gamma-ray irradiation on the optical properties of some glasses and their eventual coatings and on the mechanical properties of three glues (and a molecular adhesion technique) commonly used to attach optical components. The results of the tests are the following:

Glasses as BK7 or fused silica are not radiation resistant. The first becomes black and the second grey after a dose of 100 kGy. On the contrary, materials as BK7-G18 or optical grade fused silica (Synthetic Quartz) do not change their transmittance/reflectance properties, at least in the visible and the IR: they are very good glasses for use in high radiation ambient.

Standard triple anti-reflecting coatings stand, without major changes in performance, a dose of 100 kGy.

The study of the effect of the gamma irradiation on glues by mechanical measurements does not allow to extract definite conclusions. The data reveal motions, but, as the material used for making the probes (BK7) results very affected by the irradiation one cannot discard deformations of the glass itself. Additionally, the measurement errors are of the same order as the observed motions.

A second study about the effect of gamma-ray irradiation on glues, using optical measurements (high accuracy) and radiation resistant glasses, shows that the molecular adhesion (VACUUM) technique would be the preferable one. The inconvenient with this technique is that for large volumes there is a risk of detaching if the piece is accidentally knocked. Among NOA61, LOCTITE and MELTMOUNT the tests prefer the two firsts.

The final choice between NOA61 and LOCTITE 350 will mainly depend on their refraction index: the closer to the one of the used glass, the better. Nevertheless, the presently used probes are very small in size and, therefore, further studies, using larger size pieces would be desirable.

# References

[1] The CMS Collaboration, CMS Technical Proposal, CERN/LHCC 94-38.
[2] The CMS Collaboration, The Muon Project Technical Design Report, CERN/LHCC 98-6.
[3] The CMS Collaboration, The Tracker Project Technical Design Report, CERN/LHCC 98-6.
[4] J. Cárabe et al., Nucl. Instr. and Methods A 455 (2000) 361.

## Table captions

Table 1: Results from glue deformation (mechanical measurements, see text) due to the irradiation.
Table 2: Results from glue deformation (numbers in μrad, optical measurements, BK7-G18, see text) due to the irradiation.
Table 3: Results from glue deformation (numbers in μrad, optical measurements, Synthetic Quartz, see text) due to the irradiation.

| LOCTITE 350 | | | EPOTECNY NOA61 | | |
|---|---|---|---|---|---|
| Dose (kGy) | Angle (μrad) | r.m.s. (μrad) | Dose (kGy) | Angle (μrad) | r.m.s. (μrad) |
| 0 | 1569554 | 34 | 0 | 1569669 | 21 |
| 0 | 1569556 | 31 | 0 | 1569678 | 27 |
| 100 | 1569601 | 28 | 100 | 1569730 | 44 |
| 100 | 1569600 | 39 | 200 | 1569760 | 25 |

Table 1: Results from glue deformation (mechanical measurements, see text) due to irradiation

| Dose (kGy) | NOA61 | LOCTITE350 | MELMOUNT | VACUUM |
|---|---|---|---|---|
| 0 | 700.1 ± 2.4 | 784.5 ± 2.4 | 961.9 ± 3.4 | 2136.3 ± 2.4 |
| 50 | 700.6 ± 2.4 | 785.7 ± 2.4 | 996.8 ± 3.4 | 2139.3 ± 2.4 |
| 100 | 699.2 ± 2.4 | 785.2 ± 2.4 | 996.6 ± 3.4 | 2138.4 ± 2.4 |
| 150 | 701.6 ± 2.4 | 786.4 ± 2.4 | 996.8 ± 3.4 | 2138.9 ± 2.4 |

Table 2: Results from glue deformation (numbers in μrad, optical measurements, BK7-G18, see text) due to irradiation

| Dose (kGy) | NOA61 | LOCTITE350 | MELMOUNT | VACUUM |
|---|---|---|---|---|
| 0 | 1332.2 ± 6.3 | 2815.7 ± 6.9 | 431.0 ± 8.0 | 333.5 ± 7.6 |
| 50 | 1313.7 ± 6.0 | 2817.8 ± 6.9 | 421.3 ± 7.6 | 330.3 ± 7.6 |
| 100 | 1315.1 ± 6.0 | 2827.1 ± 7.4 | 420.6 ± 7.4 | 333.1 ± 6.9 |
| 150 | 1313.8 ± 6.0 | 2826.0 ± 7.6 | 420.8 ± 7.6 | 339.9 ± 6.9 |

Table 3: Results from glue deformation (numbers in μrad, optical measurements, Synthetic Quartz, see text) due to irradiation

## Figure captions

Fig. 1: Longitudinal view of the CMS detector showing the light paths on a ◦ plane.
Fig. 2: Scheme of the light path linking Tracker and Muon Chambers.
Fig. 3: Sketch of the modified rhomboid prism of the light source box.
Fig. 4: Drawing of the periscope prototype.
Fig. 5: Effect of the irradiation on the optical properties of two BK7-G18 probes, as a function of the light wave-length:
Fig. 6: Effect of the irradiation on standard triple anti-reflecting coatings as a function of the light wave-length:
Fig. 7: Sketch of a retro-reflector. The arrows represent the normal to the inclined faces.
Fig. 8: Photograph of one of the retro-reflectors at the DEA machine table:
up) Overall view,
down) Detail.
Fig. 9: Sketch of the set-up for the measurements of the wedge between two glued glasses with the help of a goniometer.
Fig. 10: For the BK7G18 probes (see text): transmittance (in %) as a function of the incoming wave-length before and after each irradiation step.
Fig. 11: For the Synthetic Quartz probes (see text): transmittance (in %) as a function of the incoming wave-length before and after each irradiation step.

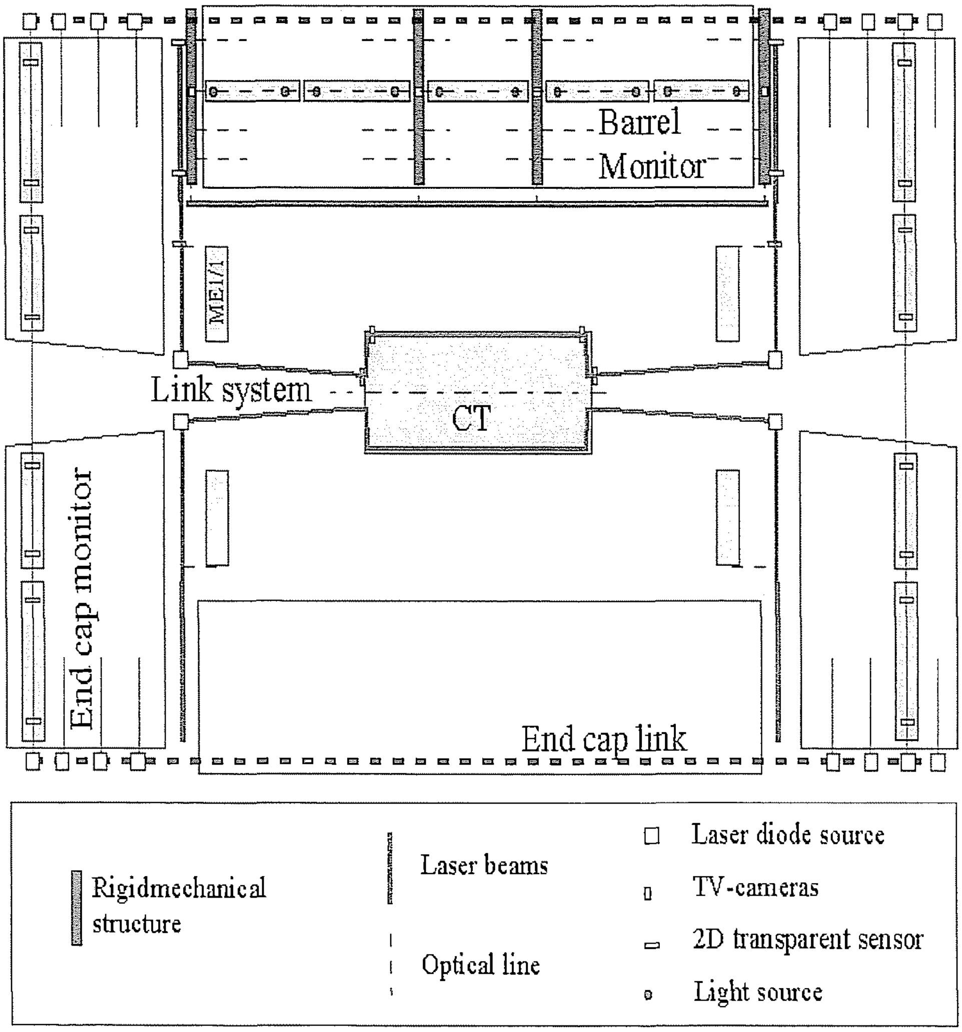
Barrel
Monitor
ME1/1
Link system
CT
End cap monitor
End cap link
Rigidmechanical structure
Laser beams
Optical line
Laser diode source
TV-cameras
2D transparent sensor
Light source

Fig. 1

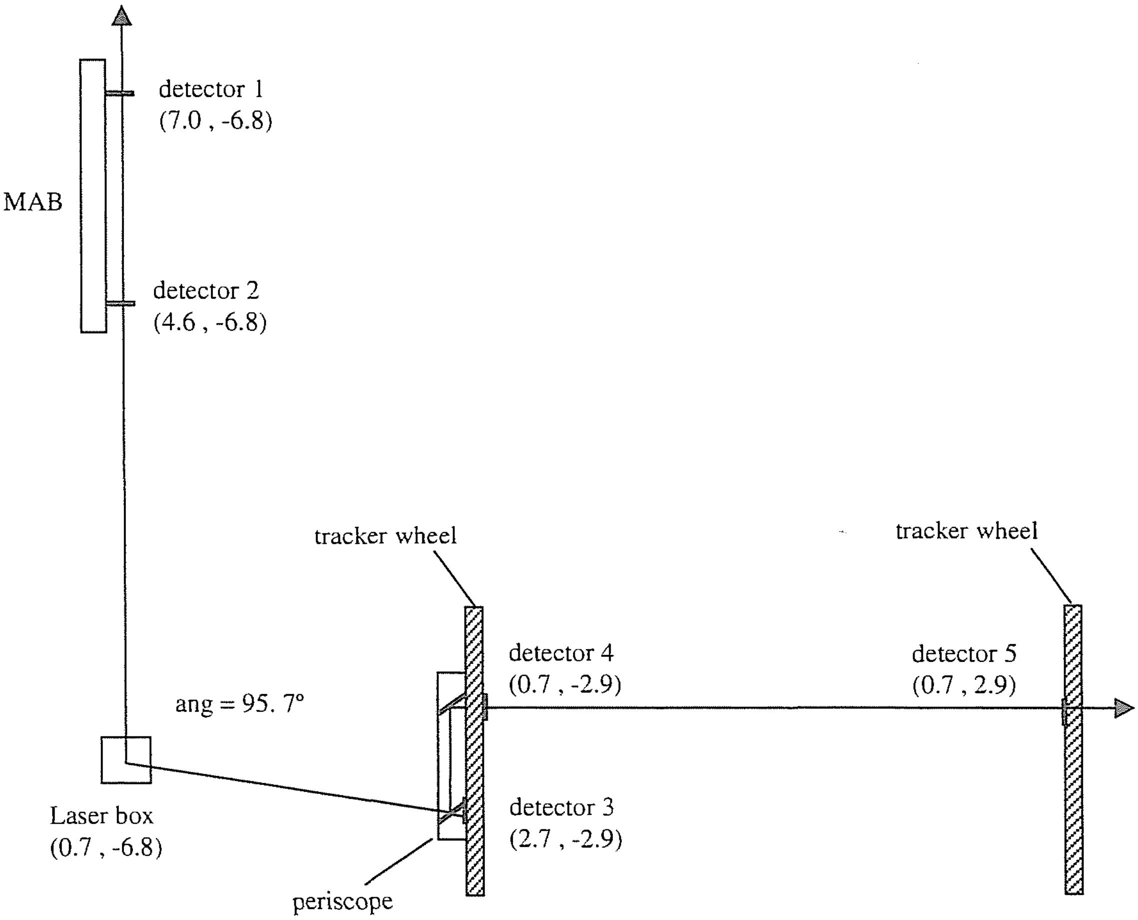
detector 1
(7.0 , -6.8)
MAB
detector 2
(4.6 , -6.8)
tracker wheel
tracker wheel
detector 4
(0.7 , -2.9)
detector 5
(0.7 , 2.9)
ang = 95. 7°
Laser box
(0.7 , -6.8)
detector 3
(2.7 , -2.9)
periscope

Fig. 2

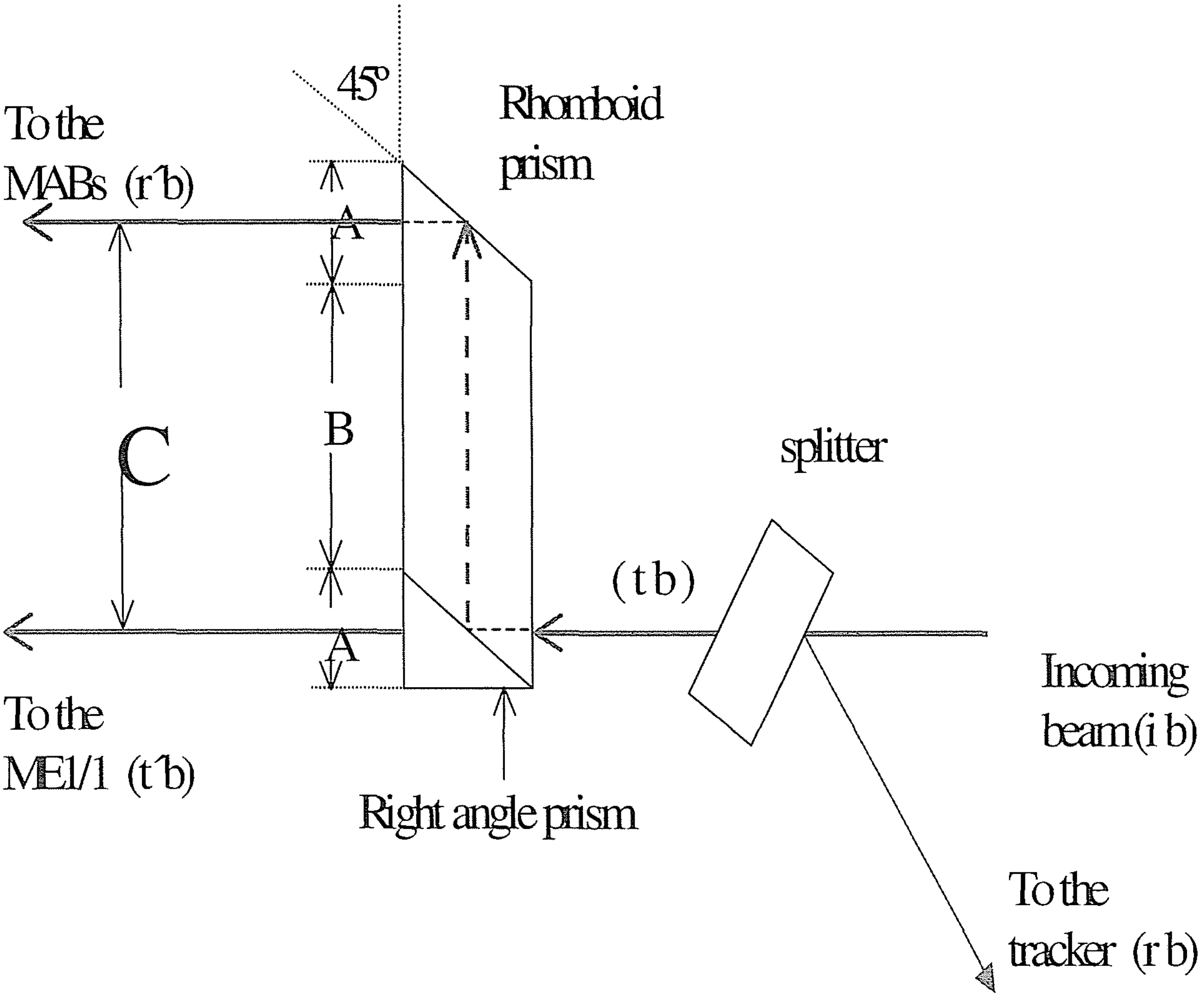
45°
To the MABs (r´b)
Rhomboid prism
A
B
C
splitter
(t b)
A
To the ME1/1 (t´b)
Incoming beam (i b)
Right angle prism
To the tracker (r b)

**Fig. 3**

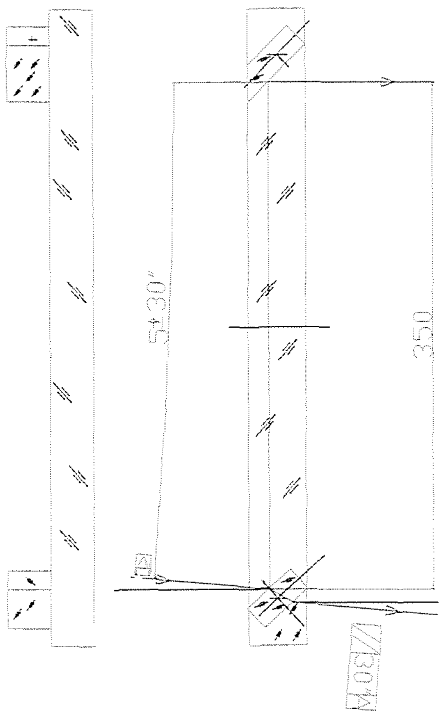

Fig. 4

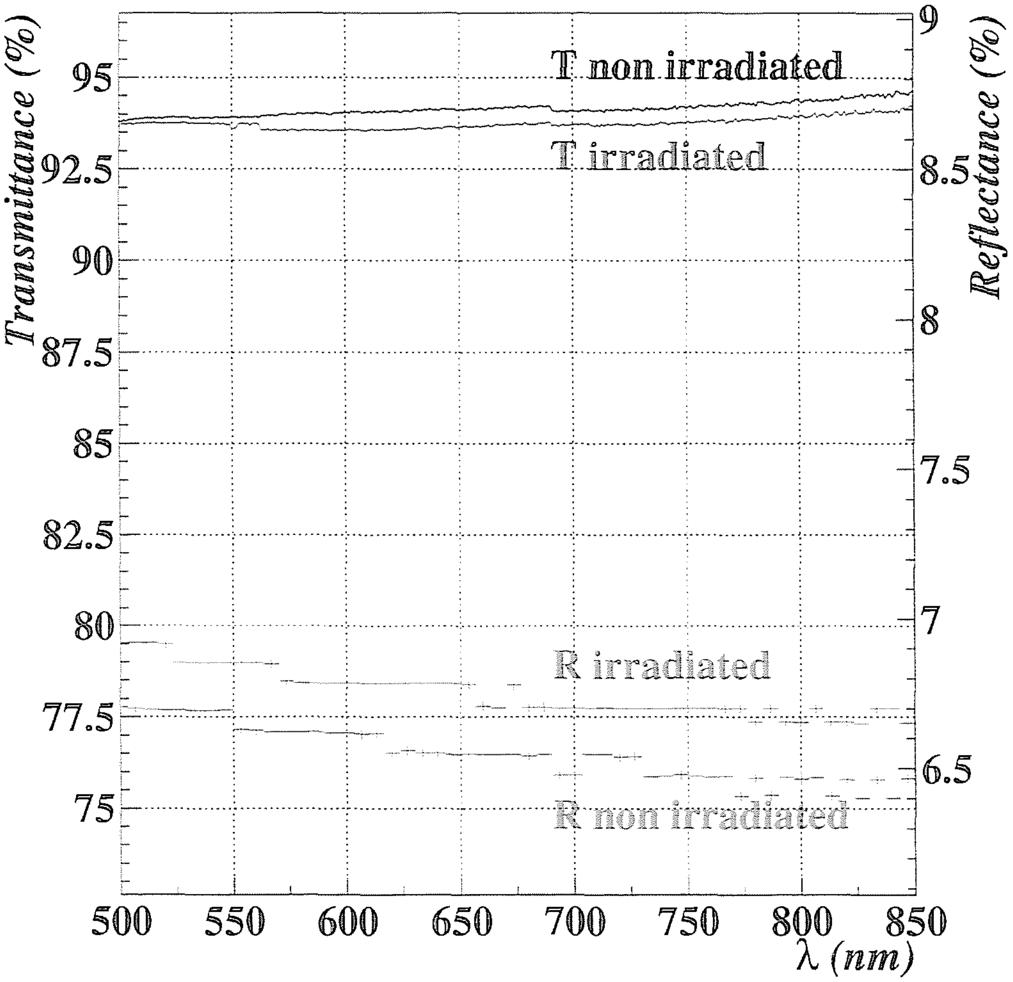
T non irradiated
T irradiated
R irradiated
R non irradiated
Transmittance (%)
Reflectance (%)
95
92.5
90
87.5
85
82.5
80
77.5
75
9
8.5
8
7.5
7
6.5
500
550
600
650
700
750
800
850
λ (nm)

Fig. 5

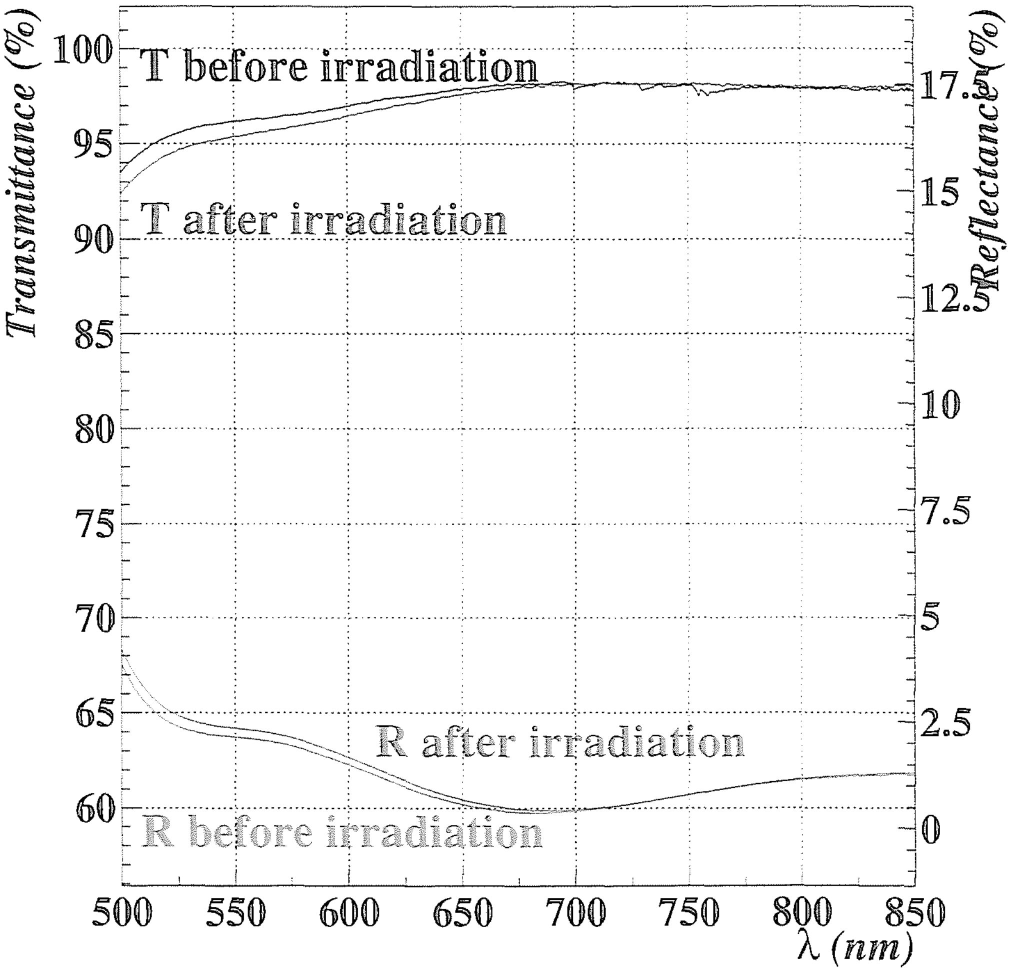
Transmittance (%)
100
95
90
85
80
75
70
65
60
T before irradiation
T after irradiation
R after irradiation
R before irradiation
Reflectance (%)
17.5
15
12.5
10
7.5
5
2.5
0
500
550
600
650
700
750
800
850
λ (nm)

Fig. 6

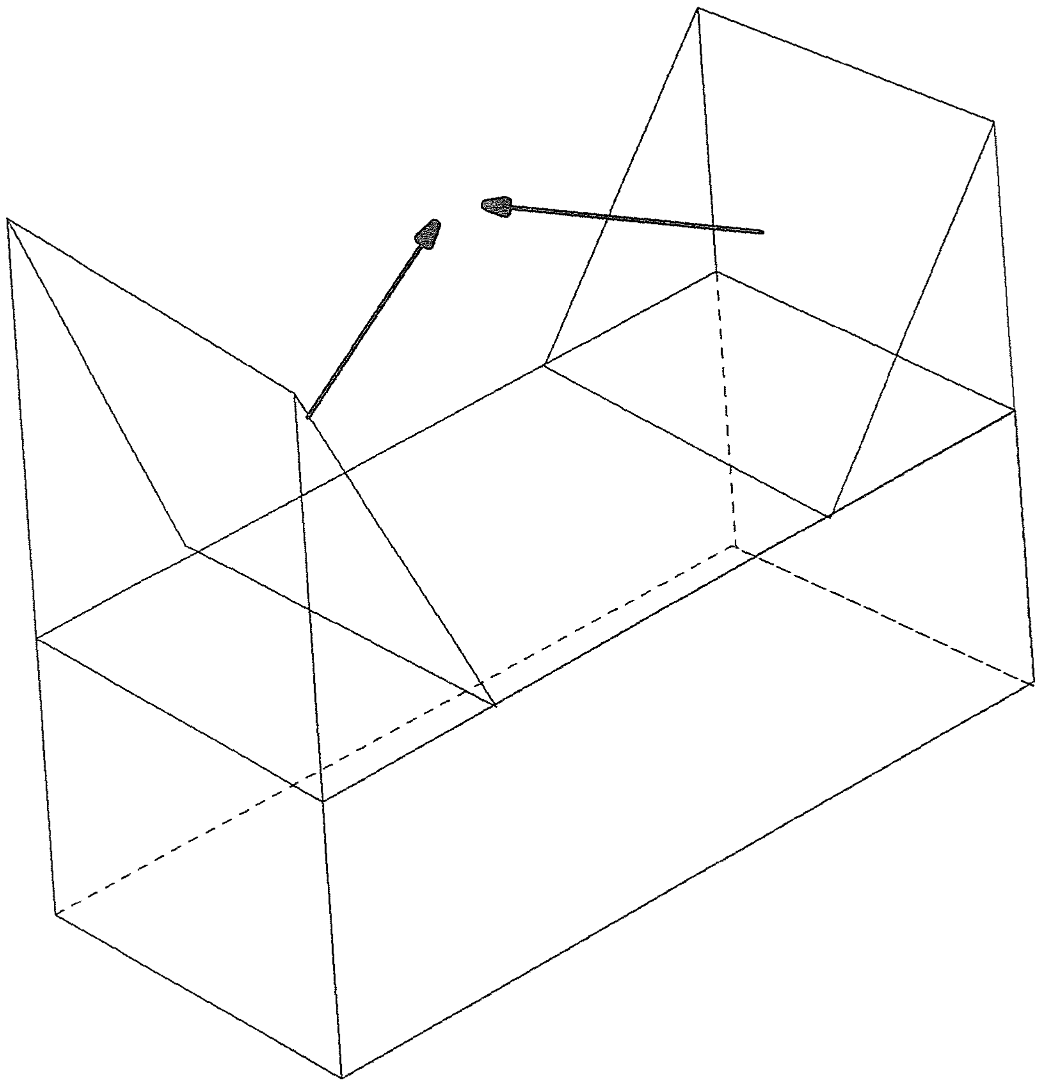

Fig. 7

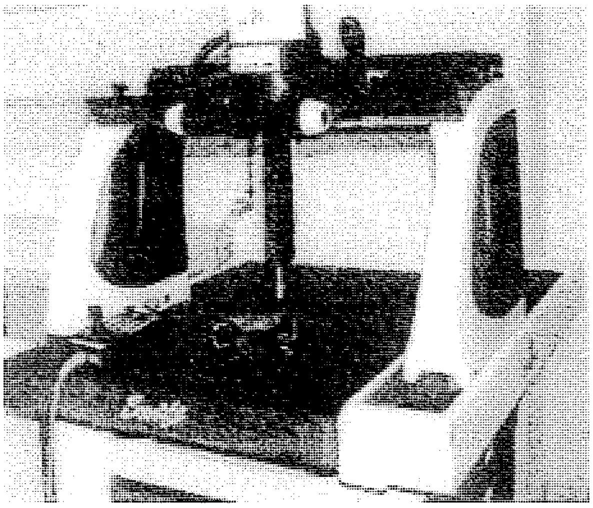

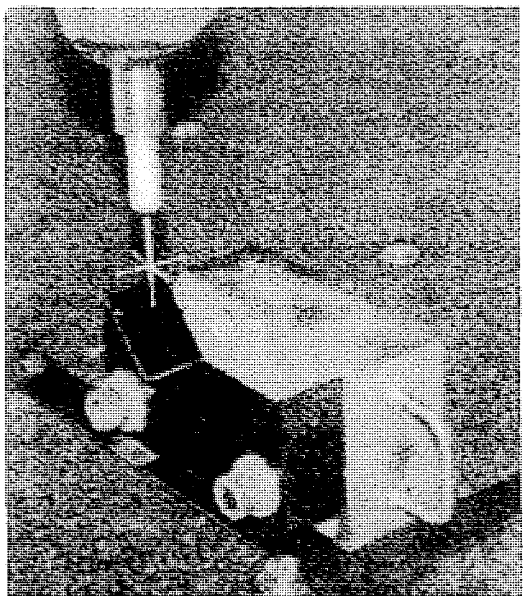

Fig. 8

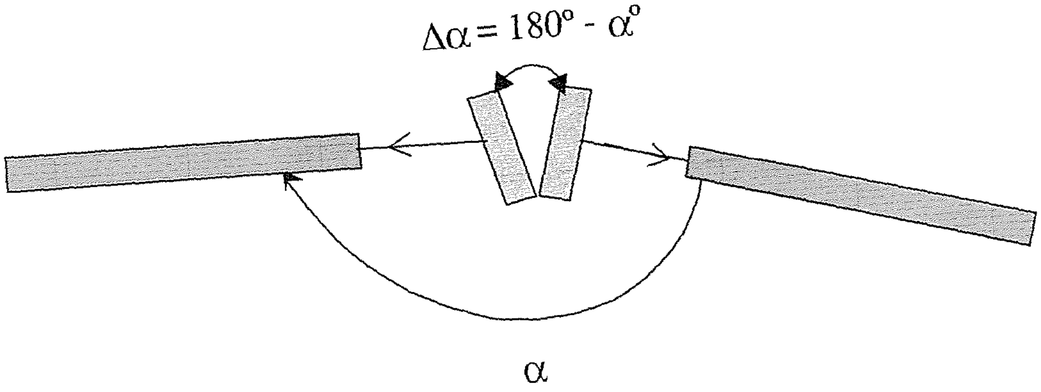

Fig. 9

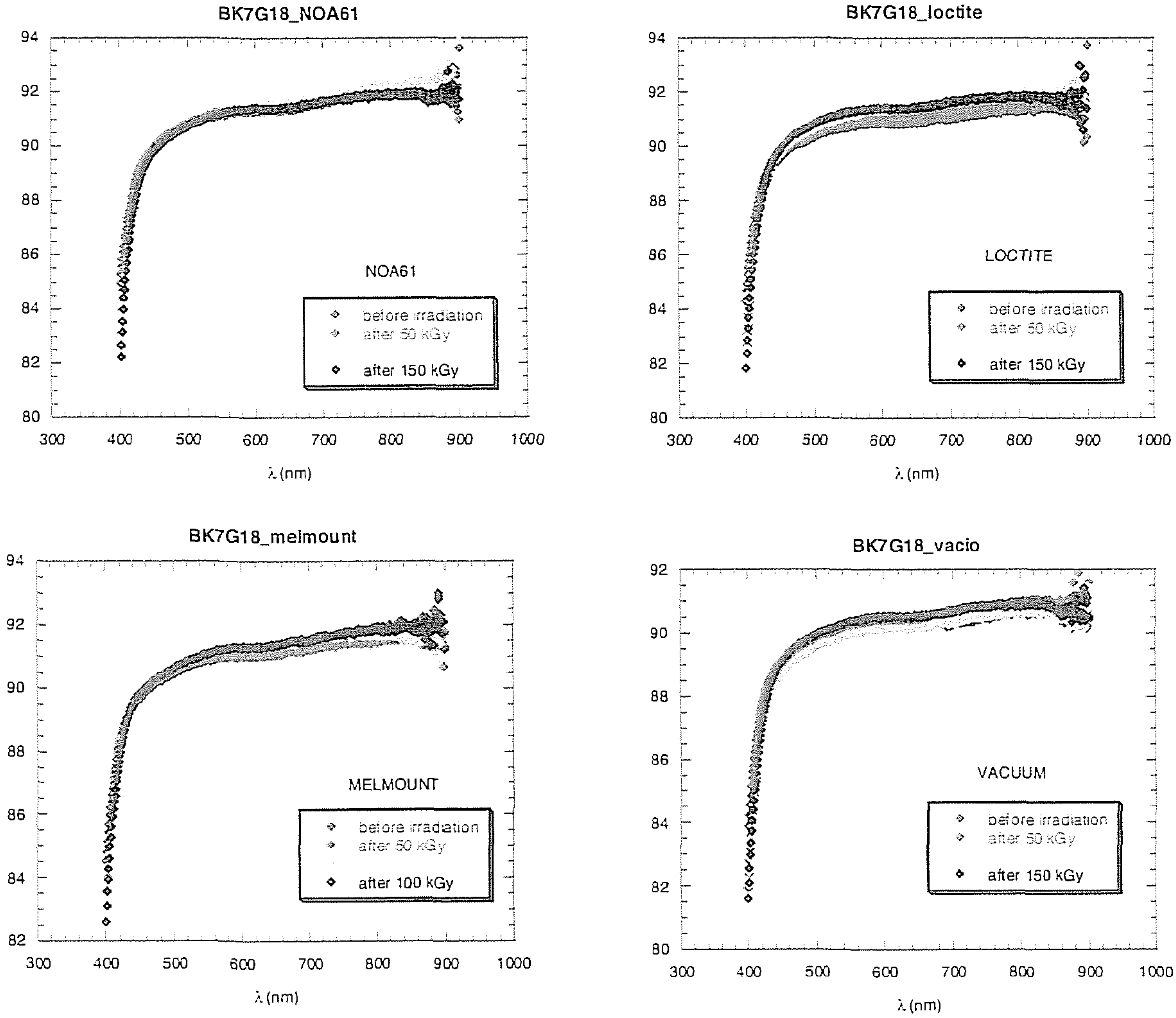
BK7G18_NOA61
NOA61
before irradiation
after 50 kGy
after 150 kGy
94
92
90
88
86
84
82
80
300
400
500
600
700
800
900
1000
λ (nm)
BK7G18_loctite
LOCTITE
before irradiation
after 50 kGy
after 150 kGy
94
92
90
88
86
84
82
80
300
400
500
600
700
800
900
1000
λ (nm)
BK7G18_melmount
MELMOUNT
before irradiation
after 50 kGy
after 100 kGy
94
92
90
88
86
84
82
300
400
500
600
700
800
900
1000
λ (nm)
BK7G18_vacio
VACUUM
before irradiation
after 50 kGy
after 150 kGy
92
90
88
86
84
82
80
300
400
500
600
700
800
900
1000
λ (nm)

Fig 10

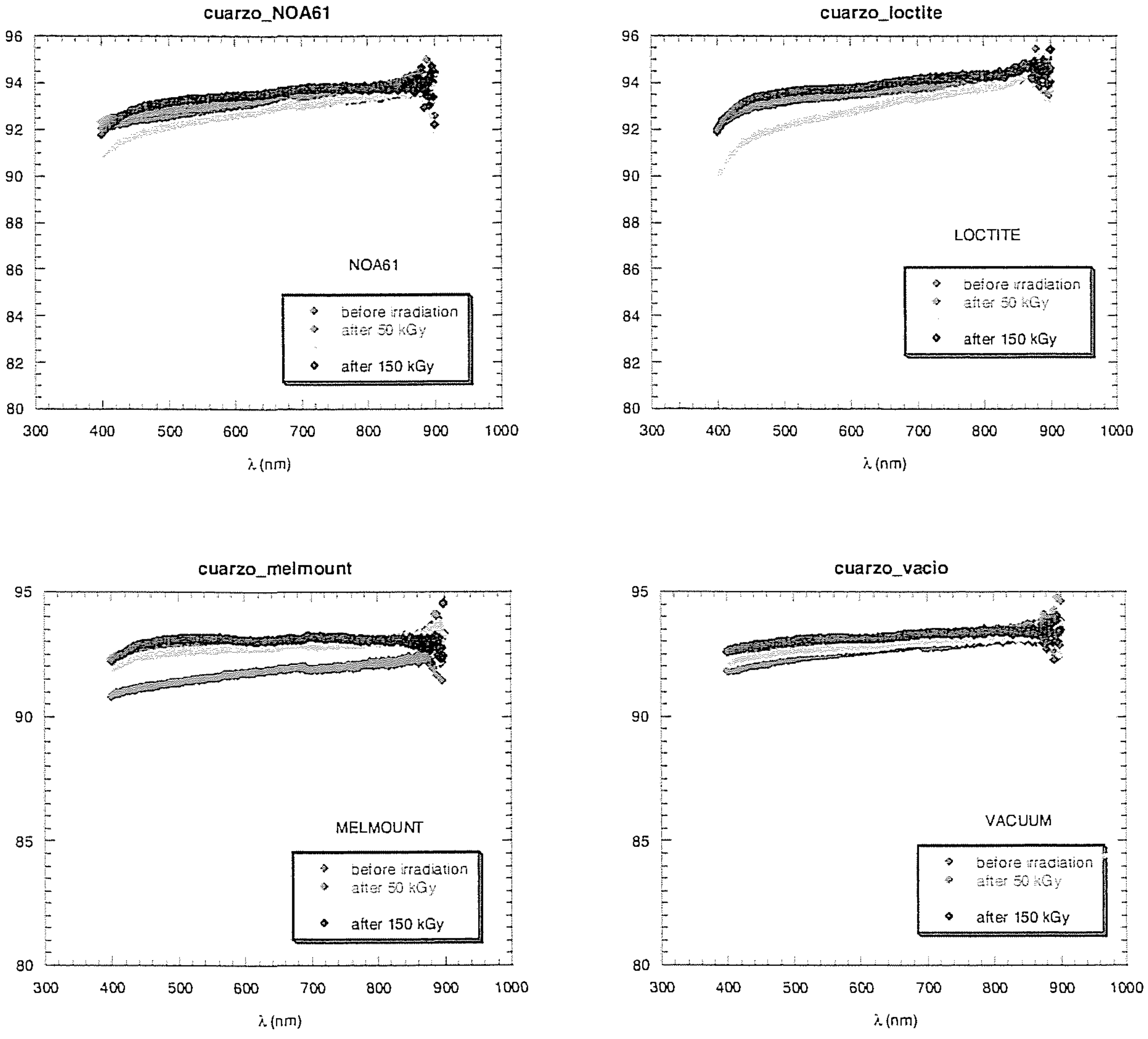
cuarzo_NOA61
96
94
92
90
88
86
84
82
80
300
400
500
600
700
800
900
1000
λ (nm)
NOA61
before irradiation
after 50 kGy
after 150 kGy
cuarzo_loctite
LOCTITE
before irradiation
after 50 kGy
after 150 kGy
λ (nm)
cuarzo_melmount
95
90
85
80
MELMOUNT
before irradiation
after 50 kGy
after 150 kGy
λ (nm)
cuarzo_vacio
VACUUM
before irradiation
after 50 kGy
after 150 kGy
λ (nm)

**Fig 11**